Arabian Journal for Science and Engineering (2022) 47:1077–1086
https://doi.org/10.1007/s13369-021-06062-z

RESEARCH ARTICLE-PHYSICS

Evaluation of the Radiation Shielding Characteristics of Several Glass Systems Using the EPICS2017 Library

F. C. Hila[1] · M. I. Sayyed[2,3] · A. M. V. Javier-Hila[1] · J. F. M. Jecong[1]

Received: 17 April 2021 / Accepted: 31 July 2021 / Published online: 18 August 2021

Abstract
In this paper, the investigation of the Electron–Photon Interaction Cross Sections 2017 (EPICS2017) library on the shielding characteristics of several glasses under various chemical systems is presented. The EPICS2017 library of ENDF/B-VIII was interpolated to calculate the mass attenuation coefficients (MACs) of selected glass systems. Results from EPICS2017 have been compared with values from experimental and theoretical methods used to evaluate the photon shielding properties. The EPICS2017 estimations strongly agreed with experimental MAC results. The MAC values from several Monte Carlo codes (Geant4, MCNP4C, MCNP5, and FLUKA) based on EPDL97 or EPDL89 strongly agreed with EPICS2017-based interpolation, within reasonable deviations. The obtained results indicate that EPICS2017 can be used to evaluate the MACs for any glass system in which there are no experimental values available at various photon energies. It was demonstrated that the linear EPICS2017 library can be a considerable tool in future photon shielding research and developments of glass systems, as a recent alternative to the widely used XCOM by NIST.

Keywords EPICS2017 library · Glasses · Gamma radiation · Shielding

1 Introduction

In the twenty-first century, technologies that utilize ionizing radiation like X-rays and gamma rays are becoming progressively more prominent. Ionizing radiation has become important in the dental and medical field, for instance, in X-ray imaging equipment for radiography. Several applications in medical treatment and medical diagnostics are reliant on gamma radiation. For instance, gamma rays are used in the sterilization of human tissue, such as in connective tissue allograft. Furthermore, ionizing radiation is used in various fields such as in energy generation, chemistry and materials science, food industry, astronomy and agriculture [1–5]. Although these radiations are excessively utilized for their many advantages, human exposure to these kinds of radiations can have dangerous consequences. This is because ionizing radiations carry a lot of energy which dissipate through several ionization cascades. Due to their tiny wavelengths, they penetrate nearly all kinds of media. Hence, thick concrete blocks or lead is used to stop their penetration. The recent studies showed that the exposure to ionizing radiation for a long time may cause vomiting, nausea, cancer, and death [6]. To protect patients and medical staff who deal directly with radiation, it is advised to remain as far away from the radioactive sources as possible, and it is advised to limit the exposure time to the radiation. In certain situations, it may not be applicable to limit the exposure time and distance. Accordingly, in order to provide more protection, radiation shields are utilized to absorb incoming radiations [7–9]. Ionizing radiation shields are special materials placed between the source of radiation and the personnel. The purpose of these shielding materials is to absorb or attenuate as much incoming radiation as possible to diminish the number of the incoming photons (i.e., intensity) to safe

✉ M. I. Sayyed
dr.mabualssayed@gmail.com

✉ J. F. M. Jecong
jmjecong@pnri.dost.gov.ph

[1] Department of Science and Technology, Philippine Nuclear Research Institute (DOST-PNRI), Commonwealth Avenue, Diliman, 1101 Quezon City, Philippines

[2] Department of Nuclear Medicine Research, Institute for Research and Medical Consultations (IRMC), Imam Abdulrahman Bin Faisal University (IAU), P.O. Box 1982, Dammam 31441, Saudi Arabia

[3] Department of Physics, Faculty of Science, Isra University, Amman, Jordan

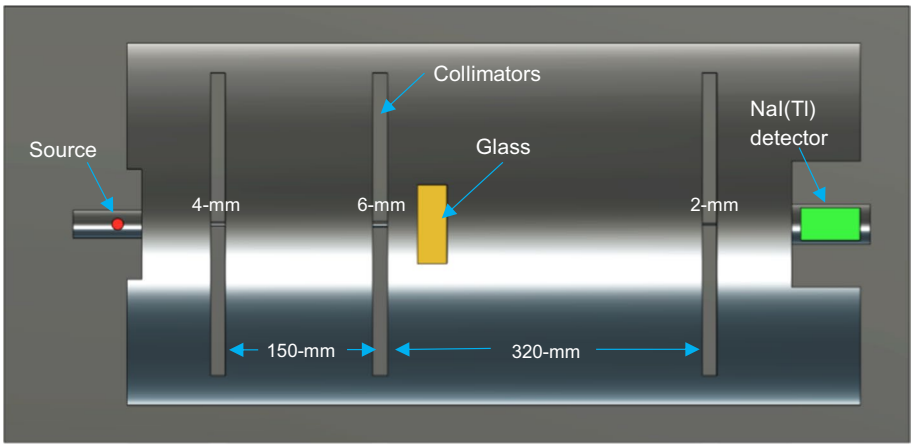

Fig. 1 Illustration of the setup in Kumar 2017 [26] for PbO–Li_2O–B_2O_3 glass system

levels [10, 11]. Thus, these reduce the harmful effects resulting from radiation that a person can be exposed to. Diverse kinds of materials are frequently utilized as ionizing radiation shields depending on their applications. Researchers in the field of radiation protection have tended to develop new types of glasses as suitable materials for radiation protection uses [12–15]. Glasses have an excellent transparency, easy method of fabrication, variety of techniques available in manufacturing, and have radiation shielding characteristics that can be enhanced easily by incorporating heavy metal oxides in the glass's formula. Accordingly, glasses are suitable materials to be used in X-ray rooms, and other medical facilities to allow employees to see the patients during medical treatments.

To evaluate the radiation shielding ability of a material, an experimental procedure can be undergone where the material is exposed to a beam of photons of known energy. The initial intensity, or number of photons, is first measured, and is compared to the amount collected at the detector. Through simple calculations, the linear and mass attenuation coefficient of the sample can be determined at these energies [16, 17]. This experimental method is often used; however, some restrictions are involved in this method. An expert in the field is necessary to undergo the experiment, and various types of equipment and radioisotopes are needed. Additionally, other factors such as the spread of COVID-19, closing many universities and research centers, complicate this process. Due to these factors, researchers use theoretical calculations to determine attenuation factors.

Theoretical estimations are essential before the preparation of the glasses, to ensure the samples are properly made and return appropriate results [18, 19]. This step is necessary prior to conducting the experiment. The most widely used theoretical estimation method is by XCOM-NIST web program. Several simulation programs are also commonly used to theoretically determine radiation shielding parameters. These include MCNP, Geant4, and others which are Monte Carlo-based methods to determine the parameters. The Monte Carlo simulation method uses a photoatomic database and random sampling to simulate the shielding values. These simulations and codes allow researchers to easily determine the parameters of their samples. The results are then compared with the values obtained from experimental methods, and if they strongly agree with each other, the researchers can continue by calculating other parameters and analyzing the results [20, 21].

The Electron–Photon Interaction Cross Sections 2017 (EPICS2017) provides the latest atomic data needed to perform coupled Electron–Photon transport calculations. This library provides partial cross sections for the elements, $Z=1$ to $Z=100$, over the range of 10 eV to 100 GeV. It is the official ENDF/B-VIII electron and photon data [22–24]. It is distinguished from its predecessors by new binding energies that will translate to new partial cross sections especially of photoelectric effect. Furthermore, the application of this library towards new and unfamiliar users has been improved by the linearization of this library. Starting from EPICS2017, all partial cross sections are now Linear–Linear interpolable. Hence, EPICS2017 is a considerable system for comparison to other libraries. Some user-based assessments of EPICS2017 have also been made [25]; nonetheless, these were assessments of the preliminary or replaced version prior to the major April 2018 update [24].

In this paper, we present the investigation of the EPICS2017 library to the shielding features of several glasses under various chemical systems. The extraction of this library was described with consideration towards the new users. Furthermore, the EPICS2017 interpolation method was compared with several experimental and theoretical methods used for characterization of photon shielding properties. With respect to Monte Carlo simulations, we mention the advantages of using the EPICS2017 library interpolations. The methods and results from this work can serve as a reference for the future photon radiation shielding evaluations.

Table 1 Compositions of selected glass systems

Glass code	Elemental composition (wt%)
$PbO–Li_2O–B_2O_3$ glass systems[a]	
PbLiB1	B(5.35); O(17.8); Pb(76.85)
PbLiB2	Li(0.46); B(5.69); O(18.93); Pb(74.93)
PbLiB3	Li(0.97); B(6.07); O(20.22); Pb(72.74)
PbLiB4	Li(1.57); B(6.51); O(21.69); Pb(70.23)
PbLiB5	Li(2.25); B(7.03); O(23.39); Pb(67.33)
PbLiB6	Li(3.06); B(7.62); O(25.39); Pb(63.93)
$Li_2O–SrO–Gd_2O_3–B_2O_3$ and $Li_2O–SrO–GdF_3–B_2O_3$ glass systems[b]	
LiSrGdB1	Li(13.94); B(13.98); O(50.62); Sr(8.46); Gd(13.01)
LiSrGdB2	Li(13.94); B(13.98); O(48.63); F(3.99); Sr(8.46); Gd(11.01)
PbO- and Bi_2O_3-influenced glass systems[c]	
PbBiG1	B(6.21); O(49.64); Si(30.38); Pb(9.28); Bi(4.48)
PbBiG2	B(20.19); O(51.31); Al(5.29); Pb(23.21)
PbBiG3	B(3.11); O(35.77); Al(5.29); Si(18.7); Pb(37.13)
PbBiG4	O(29.59); Al(5.29); Si(18.7); Pb(46.42)
PbBiG5	B(6.21); O(21.09); Pb(27.85); Bi(44.85)
$BaO–Bi_2O_3$–Borosilicate glass systems[d]	
BaBiBS1	B(1.94); O(22.96); Na(1.88); Al(2.83); Si(7); K(1.47); Ba(61.92)
BaBiBS2	B(1.48); O(19.97); Na(1.43); Al(2.16); Si(5.34); K(1.12); Ba(52.51); Bi(15.99)
BaBiBS3	B(1.14); O(17.77); Na(1.11); Al(1.67); Si(4.12); K(0.86); Ba(45.58); Bi(27.75)
BaBiBS4	B(0.88); O(16.07); Na(0.86); Al(1.29); Si(3.19); K(0.67); Ba(40.27); Bi(36.77)
BaBiBS5	B(0.68); O(14.74); Na(0.66); Al(1); Si(2.45); K(0.51); Ba(36.06); Bi(43.9)
$Li_2O–B_2O_3–P_2O_5–TeO_2$ glass systems[e]	
LiBPTe0	Li(8.82); B(2.75); O(56.94); P(31.49)
LiBPTe10	Li(7.2); B(2.24); O(50.15); P(25.7); Te(14.71)
LiBPTe20	Li(5.85); B(1.82); O(44.53); P(20.9); Te(26.9)
LiBPTe30	Li(4.72); B(1.47); O(39.78); P(16.85); Te(37.18)
LiBPTe40	Li(3.75); B(1.17); O(35.73); P(13.39); Te(45.96)
$B_2O_3–Bi_2O_3–PbO–TiO_2$ glass systems[f]	
BBPT0.0	B(7.22); O(23.16); Pb(23.07); Bi(46.54)
BBPT1.0	B(7.28); O(23.44); Ti(0.27); Pb(22.1); Bi(46.92)
BBPT2.5	B(7.37); O(23.86); Ti(0.68); Pb(20.6); Bi(47.49)
BBPT5.0	B(7.52); O(24.59); Ti(1.39); Pb(18.03); Bi(48.48)
BBPT7.5	B(7.68); O(25.35); Ti(2.13); Pb(15.34); Bi(49.51)
BBPT10.0	B(7.85); O(26.14); Ti(2.9); Pb(12.54); Bi(50.58)
$MoO_3–B_2O_3–Bi_2O_3$ glass systems[g]	
MoBiB1	B(5.32); O(23.6); Mo(9.44); Bi(61.65)
MoBiB2	B(4.36); O(21.5); Mo(8.6); Bi(65.54)
MoBiB3	B(3.56); O(19.75); Mo(7.9); Bi(68.79)
MoBiB4	B(2.88); O(18.26); Mo(7.3); Bi(71.56)
$PbO–BaO–B_2O_3$ glass systems[h]	
PbBaB10	B(15.53); O(39.36); Ba(35.83); Pb(9.28)
PbBaB20	B(15.53); O(39.04); Ba(26.87); Pb(18.57)
PbBaB30	B(15.53); O(38.71); Ba(17.91); Pb(27.85)
PbBaB40	B(15.53); O(38.38); Ba(8.96); Pb(37.13)

[a]Kumar 2017 [26]

[b]Shamshad et al. 2017 [13]

[c]Sayyed et al. 2020 [27]

[d]Bagheri et al. 2017 [28]

[e]Aşkın et al. 2019 [29]

[f]Sayyed et al. 2019 [30]

[g]Sharma et al. 2019 [31]

[h]Aşkin et al. 2019 [32]

ENDF-6 format for 1-H

(Line 170)	…	
(Line 171)	1.00000000 4.62084E-6 1.05924839 8.74720E-6 1.10597719 1.20021E-5 **10023501**	4
(Line 172)	1.14237171 1.45375E-5 1.19922131 1.84983E-5 1.25890000 2.26569E-5 **10023501**	5
(Line 173)	1.33350268 2.78564E-5 1.39234189 3.19580E-5 1.43816887 3.51530E-5 **10023501**	6
(Line 174)	1.50975292 4.01446E-5 1.58490000 4.53857E-5 1.67881736 5.19373E-5 **10023501**	7
(Line 175)	…	

Energy (eV) Cross section (barns) Element Data type

Fig. 2 A snippet of the data from EPICS2017 in ENDF-6 format for 1-H

2 Materials and Methods

2.1 Glass Systems

Several glass systems have been selected to compare the use of EPICS2017 library in the evaluation of photon attenuation capabilities. For this, Kumar 2017 [26] evaluated photon shielding characteristics of six glass samples under the PbO–Li_2O–B_2O_3 system using ^{133}Ba, ^{137}Cs, and ^{60}Co gamma sources. A visual representation of the experimental setup is shown in Fig. 1, which describes a standard narrow beam geometry using lead collimators with significant source-detector distance.

On the other hand, Shamshad et al. 2017 [13] had evaluated Li_2O–SrO–Gd_2O_3–B_2O_3 and Li_2O–SrO–GdF_3–B_2O_3 glass samples by the experimental method involving Compton scattering technique. This technique produces a spectrum of usable energies. In both aforementioned experimental methods, a NaI(Tl) detector was used with an approximate size of 2".

Numerous studies have also evaluated photon shielding of glass systems using major Monte Carlo codes. For instance, Sayyed et al. 2020 [27] evaluated the influence of PbO and Bi_2O_3 into several glass systems using MCNP5, while Bagheri et al. 2017 [28] evaluated five glass samples under BaO–Bi_2O_3–Borosilicate system using MCNP4C. Moreover, five glass samples under Li_2O–B_2O_3–P_2O_5–TeO_2 system were evaluated by Aşkın et al. 2019 [29] and six glasses under B_2O_3–Bi_2O_3–PbO–TiO_2 system by Sayyed et al. 2019 [30], both using Geant4 toolkit for narrow beam simulations. Lastly, the FLUKA code was used by Sharma et al. 2019 [31] to evaluate four glasses under MoO_3–B_2O_3–Bi_2O_3 system. This code was also used by Aşkin et al. 2019 [32] to evaluate four glasses under PbO–BaO–B_2O_3 system.

Each aforementioned glass system was considered in this work for comparative evaluation. The chemical compositions derived from each reference are detailed in Table 1.

2.2 EPICS2017 Extraction and Interpolation

The EPICS2017 library extraction was made using the version in the ENDF-6 format [33], retrieved from the IAEA-NDS. As an example, the format for the 1-H is illustrated in Fig. 2.

In this format, each partial or total cross section has its own energy grid. The partial or total cross sections (in blue) are in units of barns and are each paired with corresponding photon energies (in red) in units of eV. There are six columns of energy and cross section grids. They are read from left to right. Following these columns, the element number is declared (in yellow) where 100 corresponds to 1-H (*e.g.*, 200 for 2-He). This number is directly connected to the type of cross section or scattering factors and functions (in green). In the illustrated example, this reads as 23/501 denoting that this is for the total atomic cross sections. Furthermore, 23/502 and 23/504 are for coherent and incoherent scattering cross sections, respectively. The 23/515 and 23/517 are for pair productions in electron and nuclear fields. Lastly, the 23/534 and above are for the individual photoelectric within each subshell.

It is worth mentioning that the sum cross sections in EPICS2017 can be interpolated directly, since the library has been converted into a linearized set of data. However, the total atomic cross section σ_T may also be derived as the sum of all available partial cross sections of photoelectric, coherent and incoherent scattering, and pair production in nuclear and electron fields, and neglecting photonuclear as:

$$\sigma_T = \sigma_{PE} + \sigma_{coh} + \sigma_{incoh} + \sigma_{PP-n} + \sigma_{PP-e} \tag{1}$$

The interpolations of each partial cross sections were executed by a program similar to the spreadsheet in Hila et al. 2020 [34] but built to use the recommended linear interpolation law of EPICS2017. In this program, the atomic masses are stored for use while the input material entry is supplied by the user. After the entry, the material's partial cross sections are derived using the element partial cross sections available in the library, through the equation:

$$\sigma = \sum f_i \sigma_i \tag{2}$$

where i is each element that comprises the material (or glass for this work), f is the atom fraction for this element, σ_i is the partial cross section for the element, and σ is the partial cross section of the material.

Table 2 Comparison of MAC from EPICS2017 (ENDF/B-VIII) and experimental in Kumar 2017 [26] for PbO–Li_2O–B_2O_3 glass systems

Glass code	356 keV			662 keV			1173 keV			1332 keV		
	EPICS2017	Expt	%D	EPICS2017	Expt	%D	EPICS2017	Expt	%D	EPICS2017	Expt	%D
PbLiB1	0.2433	0.2400 ± 0.0019	1.35	0.1020	0.1010 ± 0.0016	1.00	0.06062	0.0601 ± 0.0017	0.86	0.05549	0.0551 ± 0.0016	0.71
PbLiB2	0.2396	0.2350 ± 0.0018	1.92	0.1013	0.1000 ± 0.0018	1.31	0.06052	0.0598 ± 0.0016	1.18	0.05543	0.0549 ± 0.0014	0.95
PbLiB3	0.2354	0.2330 ± 0.0022	1.02	0.1005	0.0995 ± 0.0019	1.03	0.06040	0.0598 ± 0.0015	0.99	0.05535	0.0548 ± 0.0013	1.00
PbLiB4	0.2306	0.2280 ± 0.0020	1.13	0.09963	0.0985 ± 0.0020	1.13	0.06026	0.0594 ± 0.0014	1.43	0.05527	0.0546 ± 0.0016	1.21
PbLiB5	0.2251	0.2200 ± 0.0023	2.24	0.09858	0.0971 ± 0.0021	1.50	0.06011	0.0591 ± 0.0016	1.67	0.05517	0.0542 ± 0.0015	1.76
PbLiB6	0.2185	0.2150 ± 0.0019	1.62	0.09735	0.0968 ± 0.0019	0.56	0.05992	0.0589 ± 0.0017	1.70	0.05505	0.0539 ± 0.0012	2.10

Table 3 Comparison of MAC from EPICS2017 (ENDF/B-VIII) and experimental in Shamshad et al. 2017 [13] for Li_2O–SrO–Gd_2O_3–B_2O_3 and Li_2O–SrO–GdF_3–B_2O_3 glass systems

Glass code	EPICS2017	Expt	%D	EPICS2017	Expt	%D	EPICS2017	Expt	%D	EPICS2017	Expt	%D
	229.96 keV			257.48 keV			290.98 keV			338.83 keV		
LiSrGdB1	0.1562	0.1663 ± 0.0025	6.49	0.1398	0.1379 ± 0.0034	1.38	0.1257	0.1260 ± 0.0014	0.22	0.1120	0.1156 ± 0.0023	3.19
LiSrGdB2	0.1501	0.1556 ± 0.0027	3.66	0.1354	0.1382 ± 0.0003	2.07	0.1226	0.1249 ± 0.0034	1.91	0.1099	0.1093 ± 0.0024	0.59
	409.42 keV			482.4 keV			569.74 keV			662 keV		
LiSrGdB1	0.0989	0.1023 ± 0.0026	3.48	0.0897	0.0919 ± 0.0023	2.45	0.0817	0.0839 ± 0.0023	2.65	0.0755	0.0767 ± 0.0006	1.62
LiSrGdB2	0.0976	0.0986 ± 0.0026	1.01	0.0889	0.0913 ± 0.0023	2.69	0.0812	0.0843 ± 0.0023	3.77	0.0752	0.0754 ± 0.0004	0.32

Table 4 Comparison of MAC from EPICS2017 (ENDF/B-VIII) and MCNP5 simulations in Sayyed et al. 2020 [27] for PbO- and Bi_2O_3-influenced glass systems

Energy (MeV)	PbBiG1			PbBiG2			PbBiG3			PbBiG4			PbBiG5		
	EPICS2017	MCNP5	%D	EPICS2017	MCNP5	%D	EPICS2017	MCNP5	%D	EPICS2017	MCNP5	%D	EPICS2017	MCNP5	%D
0.015	19.599	19.607	0.04	27.258	27.283	0.09	44.302	44.585	0.64	54.492	54.787	0.54	83.321	83.369	0.06
0.02	13.801	13.787	0.10	20.666	20.644	0.11	33.303	33.372	0.21	41.231	41.293	0.15	64.196	64.130	0.10
0.04	2.3559	2.3510	0.21	3.5298	3.5230	0.19	5.5887	5.5910	0.04	6.8993	6.8990	0.00	10.7661	10.7460	0.19
0.06	0.8974	0.8970	0.04	1.3001	1.3000	0.00	1.9968	2.0000	0.16	2.4423	2.4460	0.15	3.7670	3.7650	0.05
0.08	0.4894	0.4910	0.33	0.6732	0.6770	0.56	0.9918	0.9990	0.73	1.1955	1.2040	0.71	1.8052	1.8150	0.54
0.4	0.1144	0.1140	0.33	0.1256	0.1250	0.50	0.1460	0.1460	0.03	0.1588	0.1590	0.10	0.1973	0.2060	4.41
0.8	0.0730	0.0730	0.06	0.0737	0.0740	0.44	0.0770	0.0770	0.03	0.0788	0.0790	0.22	0.0840	0.0840	0.00
1	0.0643	0.0640	0.53	0.0642	0.0640	0.31	0.0660	0.0650	1.51	0.0668	0.0650	2.70	0.0690	0.0670	2.93
4	0.0327	0.0330	0.93	0.0329	0.0330	0.40	0.0352	0.0350	0.48	0.0363	0.0360	0.77	0.0389	0.0390	0.23
8	0.0267	0.0270	1.25	0.0276	0.0280	1.36	0.0321	0.0320	0.33	0.0344	0.0350	1.62	0.0401	0.0400	0.35
10	0.0258	0.0260	0.95	0.0270	0.0270	0.09	0.0323	0.0320	0.79	0.0350	0.0350	0.10	0.0418	0.0420	0.40
15	0.0251	0.0250	0.43	0.0268	0.0270	0.60	0.0337	0.0340	1.01	0.0373	0.0370	0.79	0.0462	0.0460	0.51

Finally, the relationship of the total atomic cross section to the mass attenuation coefficient can be derived as follows:

$$\frac{\mu}{\rho} = \sigma_T \frac{N_A}{\sum f_i A_i} \tag{3}$$

where A_i is the atomic mass of the ith element and N_A is Avogadro's number.

3 Results and Discussion

A comparison of EPICS2017-based mass attenuation coefficients and experimentally determined ones is described in Tables 2 and 3. The experimental data in Table 2 are from Kumar 2017 [26] who evaluated the PbO–Li_2O–B_2O_3 glass systems using a transmission beam geometry with several cascaded lead collimators. An agreement was shown between the EPICS2017-based interpolated results and the experimental values. For this comparison, the deviation was found to be highest at 2.2% for the 356 keV gamma ray incident in PbLiB5 glass. Furthermore, the experimental data in Table 3 show the evaluated mass attenuation coefficients for Li_2O–SrO–Gd_2O_3–B_2O_3 and Li_2O–SrO–GdF_3–B_2O_3 by Shamshad et al. 2017 [13]. Their study used the Compton scattering technique to vary the gamma ray energies. Hence, the energies reported were inevitably subjected to uncertainties which will translate in the comparison of attenuation coefficients. As shown by Table 3, there is a larger difference for this comparison due to the additional uncertainties. The maximum deviations were 6.5% in 229.96 keV for LiSrGdB1 and 3.8% in 569.74 keV for LiSrGdB2. Majority of the experimentally determined mass attenuation coefficients were lower than the theoretical due to counting statistics, sample density and geometry, and the deviations from narrow beam geometry. Nevertheless, reasonable agreements were found between the EPICS2017-based values in comparison with the experimental results.

Comparisons of simulated mass attenuation coefficients using MCNP codes are described in Tables 4 and 5. In Table 4, comparative results are shown between EPICS2017 interpolated results versus MCNP5 simulations, for several PbO- and Bi_2O_3-influenced glasses taken from Sayyed et al. 2020 [27]. This comparison is made in a broad energy range of 15 keV to 15 MeV. Good agreements were derived from these results for most of the energies considered. Furthermore, Table 5 shows comparisons for BaO–Bi_2O_3–Borosilicate glass systems using MCNP4C taken from Bagheri et al. 2017 [28]. This comparison is for the gamma energies of ^{133}Ba, ^{137}Cs, and ^{60}Co. There are slightly higher values for the simulated attenuation coefficients as compared to the EPICS2017 which may be due to deviations from narrow beam geometry of the simulation models used. It is

Table 5 Comparison of MAC from EPICS2017 (ENDF/B-VIII) and MCNP4C simulations in Bagheri et al. 2017 [28] for $BaO–Bi_2O_3$–borosilicate glass systems

Glass code	662 keV			1173 keV			1332 keV		
	EPICS2017	MCNP4C	%D	EPICS2017	MCNP4C	%D	EPICS2017	MCNP4C	%D
BaBiBS1	0.0771	0.0763	1.08	0.0546	0.0543	0.47	0.0509	0.0505	0.76
BaBiBS2	0.0828	0.0816	1.41	0.0558	0.0555	0.52	0.0518	0.0512	1.14
BaBiBS3	0.0869	0.0857	1.40	0.0567	0.0560	1.23	0.0525	0.0519	1.07
BaBiBS4	0.0901	0.0888	1.44	0.0574	0.0570	0.69	0.0530	0.0523	1.26
BaBiBS5	0.0926	0.0909	1.85	0.0579	0.0575	0.77	0.0534	0.0527	1.26

Table 6 Comparison of MAC from EPICS2017 (ENDF/B-VIII) and Geant4 simulations in Aşkın et al. 2019 [29] for $Li_2O–B_2O_3–P_2O_5–TeO_2$ glass systems

Glass code	356 keV			662 keV			1173 keV			1332 keV		
	EPICS2017	Geant4	%D	EPICS2017	Geant4	%D	EPICS2017	Geant4	%D	EPICS2017	Geant4	%D
LiBPTe0	0.0980	0.1021	4.15	0.0755	0.0817	8.28	0.0574	0.0554	3.43	0.0537	0.0525	2.32
LiBPTe10	0.1033	0.1024	0.84	0.0754	0.0756	0.32	0.0565	0.0542	4.13	0.0529	0.0536	1.27
LiBPTe20	0.1076	0.1080	0.36	0.0753	0.0761	1.09	0.0558	0.0569	1.89	0.0522	0.0503	3.73
LiBPTe30	0.1113	0.1152	3.53	0.0752	0.0773	2.77	0.0553	0.0552	0.11	0.0517	0.0510	1.31
LiBPTe40	0.1144	0.1114	2.62	0.0752	0.0733	2.47	0.0548	0.0554	1.16	0.0512	0.0517	1.00

notable that the MCNP5 is based on the EPDL97, while the MCNP4C is based on EPDL89. Both are officially superseded by the EPICS2017, and hence the values derived from the latter are considered more accurate in general.

A second comparison of simulated mass attenuation coefficients toward the EPICS2017-based interpolations is shown in Tables 6 and 7, for several gamma ray energies using the simulation toolkit Geant4. Table 6 shows the mass attenuation coefficients using the $Li_2O–B_2O_3–P_2O_5–TeO_2$ glass systems from Aşkın et al. 2019 [29], while Table 7 shows evaluations for $B_2O_3–Bi_2O_3–PbO–TiO_2$ from Sayyed et al. 2019 [30], taken for several discrete gamma energies. These results show comparable agreement between both methods. Nevertheless, it is important to note that the current Geant4 low energy electromagnetic is also derived from the Livermore data library EPDL97.

The FLUKA code which also derives from the EPDL97 has been compared to EPICS2017 based results. Tables 8 and 9 show the FLUKA simulated attenuation coefficients in several gamma energies for glass systems of $MoO_3–B_2O_3–Bi_2O_3$ and $PbO–BaO–B_2O_3$, respectively. The set of comparison for these glasses show the best agreement between all simulated attenuation coefficients versus the EPICS2017 derived values. Since FLUKA uses similar photoatomic libraries as most of the codes previously described, the closeness of the FLUKA comparison is likely attributed to good geometry of the simulation models as well as large quantities of simulation source particles used.

Several glass systems have been studied and proposed in the literature, which have certain advantages and disadvantages over others particularly in cost, optical transparency, mechanical properties, toxicity, and gamma ray shielding characteristics. In glass chemical compositions, the incorporation of heavy oxides generally increases the shielding capabilities at the possible expense or degradation of other characteristics. Conveniently, several characteristics of these materials can be theoretically tested, such as its radiation shielding characteristics. Hence, an efficient and accurate method of obtaining the gamma shielding characteristics is of importance for these widely used materials.

The intercomparisons showed an overall good agreement between the latest EPICS2017 library and several experimental and theoretical methods. It is notable that the values derived from EPICS2017 may present desirable results for these glasses. This is because most Monte Carlo codes, under the commonly used simulation models, may also derive deviations from narrow beam geometry. Furthermore, the Monte Carlo random sampling method involves obtaining the mean free paths of the glasses prior to simulations, using the built-in photoatomic data library. However, the photoatomic data libraries installed in modern Monte Carlo codes are likely the predecessors of EPICS2017. In

Table 7 Comparison of MAC from EPICS2017 (ENDF/B-VIII) and Geant4 simulations in Sayyed et al. 2019 [30] for B_2O_3–Bi_2O_3–PbO–TiO_2 glass systems

Glass code	356 keV			662 keV			1173 keV			1330 keV			2510 keV		
	EPICS2017	Geant4	%D	EPICS2017	Geant4	%D	EPICS2017	Geant4	%D	EPICS2017	Geant4	%D	EPICS2017	Geant4	%D
BBPT0.0	0.2338	0.2393	2.35	0.1006	0.1045	3.83	0.0607	0.0595	2.04	0.0557	0.0547	1.77	0.0421	0.0419	0.49
BBPT1.0	0.2327	0.2387	2.58	0.1004	0.1038	3.35	0.0607	0.0593	2.33	0.0557	0.0545	2.10	0.0421	0.0418	0.67
BBPT2.5	0.2310	0.2380	3.03	0.1001	0.1031	2.98	0.0607	0.0591	2.59	0.0556	0.0542	2.60	0.0420	0.0415	1.28
BBPT5.0	0.2281	0.2365	3.69	0.0996	0.1020	2.43	0.0606	0.0589	2.80	0.0556	0.0540	2.88	0.0420	0.0414	1.34
BBPT7.5	0.2250	0.2348	4.34	0.0990	0.1012	2.21	0.0605	0.0585	3.34	0.0556	0.0538	3.17	0.0419	0.0413	1.40
BBPT10.0	0.2218	0.2305	3.90	0.0984	0.1005	2.11	0.0604	0.0578	4.37	0.0555	0.0534	3.80	0.0418	0.0410	1.93

retrospect, some amount of time is needed to adopt new libraries into existing Monte Carlo software. Codes such as PHITS, FLUKA, and Geant4 are still based on the preceded EPDL97, and the latest MCNP6.2 is based on EPICS2014. Apart from accuracy of cross sections and absorption edge energies, one major difference between EPICS2017 and its predecessors is its construction as a linearly interpolable library. Hence, it is made easier for unfamiliar users to extract this new system with less risk of producing inaccurate data. Furthermore, the EPICS2017 is freely downloadable at present, and is hence favorable for users who do not have license to the major Monte Carlo software. Since glass systems are currently prevalent in scientific research, this therefore makes the EPICS2017 a progressive tool for photon radiation shielding and developments for this widely used material.

4 Conclusion

This study has compared the interpolated mass attenuation coefficients from experimental and theoretical simulation methods with the library interpolation method via the EPICS2017 system. The EPICS2017 has been interpolated using the recommended linear scheme, using a built program that stores the partial cross sections. The details of the extraction have been described for unfamiliar users. The results for the experimental method were shown to be in agreement with the EPICS2017-based interpolations. This includes the comparison using a discrete energy gamma source transmission setup, as well as a variable energy gamma source produced via the Compton scattering technique. Furthermore, the results for multiple glass systems evaluated using different Monte Carlo codes have shown good agreement with EPICS2017. However, several divergences were found between simulated and interpolated mass attenuation coefficients. Nevertheless, this is rooted from the deviations from narrow beam geometry of the simulation models, from Monte Carlo sampling statistics, and deviations from the photoatomic libraries of the simulation codes versus EPICS2017. Since the latter is designed specifically to replace Monte Carlo code libraries, it is therefore concluded that the EPICS2017 system is a progressive

Table 8 Comparison of MAC from EPICS2017 (ENDF/B-VIII) and FLUKA simulations in Sharma et al. 2019 [31] for MoO_3–B_2O_3–Bi_2O_3 glass systems

Glass code	356 keV			662 keV			1173 keV			1330 keV		
	EPICS2017	FLUKA	%D	EPICS2017	FLUKA	%D	EPICS2017	FLUKA	%D	EPICS2017	FLUKA	%D
MoBiB1	0.2219	0.2213	0.27	0.0982	0.0977	0.49	0.0602	0.0603	0.12	0.0553	0.0553	0.03
MoBiB2	0.2295	0.2287	0.33	0.0996	0.0992	0.43	0.0605	0.0604	0.09	0.0555	0.0555	0.07
MoBiB3	0.2358	0.2350	0.33	0.1008	0.1005	0.34	0.0606	0.0604	0.41	0.0556	0.0556	0.03
MoBiB4	0.2412	0.2397	0.61	0.1019	0.1015	0.36	0.0608	0.0605	0.51	0.0557	0.0555	0.34

Table 9 Comparison of MAC from EPICS2017 (ENDF/B-VIII) and FLUKA simulations in Aşkin et al. 2019 [32] for PbO–BaO–B_2O_3 glass systems

Glass code	356 keV			662 keV			1173 keV			1332 keV		
	EPICS2017	FLUKA	%D	EPICS2017	FLUKA	%D	EPICS2017	FLUKA	%D	EPICS2017	FLUKA	%D
PbBaB10	0.1330	0.1323	0.53	0.0794	0.0791	0.44	0.0560	0.0558	0.39	0.0522	0.0520	0.36
PbBaB20	0.1462	0.1457	0.32	0.0825	0.0823	0.19	0.0568	0.0656	15.40	0.0528	0.0526	0.46
PbBaB30	0.1593	0.1587	0.39	0.0855	0.0850	0.54	0.0577	0.0574	0.48	0.0535	0.0531	0.74
PbBaB40	0.1725	0.1716	0.50	0.0885	0.0881	0.42	0.0585	0.0582	0.52	0.0541	0.0539	0.45

instrument in future photon shielding research and developments of glass materials.

References

1. Al-Hadeethi, Y.; Sayyed, M.I.: $BaO–Li_2O–B_2O_3$ glass systems: potential utilization in gamma radiation protection. Prog. Nucl. Energy **129**, 103511 (2020). https://doi.org/10.1016/j.pnucene.2020.103511
2. Jecong, J.F.M.; Hila, F.C.; Dingle, C.A.M.; Astronomo, A.A.; Gatchalian, R.D.E.; Romallosa, K.M.D.; Guillermo, N.R.D.: Development and validation of a Serpent-2 model for the former 3 MW TRIGA core configuration of the Philippine Research Reactor-1. Philipp. J. Sci. **149**(S1), 87–92 (2020)
3. Mhareb, M.H.A.: Physical, optical and shielding features of $Li_2O–B_2O_3–MgO–Er_2O_3$ glasses co-doped of Sm_2O_3. Appl. Phys. A. (2020). https://doi.org/10.1007/s00339-019-3262-9
4. Manjunatha, H.C.; Seenappa, L.; Chandrika, B.M.; Hanumantharayappa, C.: A study of photon interaction parameters in barium compounds. Ann. Nucl. Energy **109**, 310–317 (2017). https://doi.org/10.1016/j.anucene.2017.05.042
5. Al-Hadeethi, Y.; Sayyed, M.I.; Rammah, Y.S.: Fabrication, optical, structural and gamma radiation shielding characterizations of $GeO_2–PbO–Al_2O_3–CaO$ glasses. Ceram. Int. **46**, 2055–2062 (2020). https://doi.org/10.1016/j.ceramint.2019.09.185
6. Khalifa, J.; François, S.; Rancoule, C.; Riccobono, D.; Magné, N.; Drouet, M.; Chargari, C.: Gene therapy and cell therapy for the management of radiation damages to healthy tissues: rationale and early results. Cancer/Radiothérapie **23**, 449–465 (2019). https://doi.org/10.1016/j.canrad.2019.06.002
7. Obaid, S.S.; Gaikwad, D.K.; Pawar, P.P.: Determination of gamma ray shielding parameters of rocks and concrete. Radiat. Phys. Chem. **144**, 356–360 (2018). https://doi.org/10.1016/j.radphyschem.2017.09.022
8. Dong, M.; Xue, X.; Kumar, A.; Yang, H.; Sayyed, M.I.; Liu, S.; Bu, E.: A novel method of utilization of hot dip galvanizing slag using the heat waste from itself for protection from radiation. J. Hazard. Mater. **344**, 602–614 (2018). https://doi.org/10.1016/j.jhazmat.2017.10.066
9. Singh, V.P.; Badiger, N.M.: Shielding efficiency of lead borate and nickel borate glasses for gamma rays and neutrons. Glass Phys. Chem. **41**, 276–283 (2015). https://doi.org/10.1134/s1087659615030177
10. Aşkın, A.: Assesment of the gamma and neutron shielding capabilities of the boro-tellurite glass quaternary containing heavy metal oxide using Geant4 and Phy-X/PSD database. Ceram. Int. **46**, 14090–14096 (2020). https://doi.org/10.1016/j.ceramint.2020.02.209
11. Al-Hadeethi, Y.; Sayyed, M.I.; Mohammed, H.; Rimondini, L.: X-ray photons attenuation characteristics for two tellurite based glass systems at dental diagnostic energies. Ceram. Int. **46**, 251–257 (2020). https://doi.org/10.1016/j.ceramint.2019.08.258
12. Cheewasukhanont, W.; Limkitjaroenporn, P.; Kothan, S.; Kedkaew, C.; Kaewkhao, J.: The effect of particle size on radiation shielding properties for bismuth borosilicate glass. Radiat. Phys. Chem. **172**, 108791 (2020). https://doi.org/10.1016/j.radphyschem.2020.108791
13. Shamshad, L.; Rooh, G.; Limkitjaroenporn, P.; Srisittipokakun, N.; Chaiphaksa, W.; Kim, H.J.; Kaewkhao, J.: A comparative study of gadolinium based oxide and oxyfluoride glasses as low energy radiation shielding materials. Prog. Nucl. Energy **97**, 53–59 (2017). https://doi.org/10.1016/j.pnucene.2016.12.014
14. Al-Hadeethi, Y.; Sayyed, M.I.: A comprehensive study on the effect of TeO_2 on the radiation shielding properties of $TeO_2–B_2O_3–Bi_2O_3–LiF–SrCl_2$ glass system using Phy-X/PSD software. Ceram. Int. **46**, 6136–6140 (2020). https://doi.org/10.1016/j.ceramint.2019.11.078
15. Rachniyom, W.; Chaiphaksa, W.; Limkitjaroeanporn, P.; Tuschaoen, S.; Sangwaranatee, N.; Kaewkhao, J.: Effect of Bi_2O_3 on radiation shielding properties of glasses from coal fly ash. Mater. Today Proc. **5**, 14046–14051 (2018). https://doi.org/10.1016/j.matpr.2018.02.059

16. Halimah, M.K.; Azuraida, A.; Ishak, M.; Hasnimulyati, L.: Influence of bismuth oxide on gamma radiation shielding properties of boro-tellurite glass. J. Non-Cryst. Solids **512**, 140–147 (2019). https://doi.org/10.1016/j.jnoncrysol.2019.03.004
17. Aygün, B.: High alloyed new stainless steel shielding material for gamma and fast neutron radiation. Nucl. Eng. Technol. **52**, 647–653 (2020). https://doi.org/10.1016/j.net.2019.08.017
18. Abouhaswa, A.S.; Mhareb, M.H.A.; Alalawi, A.; Al-Buriahi, M.S.: Physical, structural, optical, and radiation shielding properties of B_2O_3–$20Bi_2O_3$–$20Na_2O_2$–SB_2O_3 glasses: role of SB_2O_3. J. Non-Cryst. Solids **543**, 120130 (2020). https://doi.org/10.1016/j.jnoncrysol.2020.120130
19. Hendi, A.A.; Rashad, M.; Sayyed, M.I.: Gamma radiation shielding study of tellurite glasses containing V_2O_5 and Bi_2O_3 using Geant4 code. Ceram. Int. **46**, 28870–28876 (2020). https://doi.org/10.1016/j.ceramint.2020.08.053
20. Alajerami, Y.S.; Drabold, D.; Mhareb, M.H.A.; Cimatu, K.L.A.; Chen, G.; Kurudirek, M.: Radiation shielding properties of bismuth borate glasses doped with different concentrations of cadmium oxides. Ceram. Int. **46**, 12718–12726 (2020). https://doi.org/10.1016/j.ceramint.2020.02.039
21. Aygün, B.; Şakar, E.; Singh, V.P.; Sayyed, M.I.; Korkut, T.; Karabulut, A.: Experimental and Monte Carlo simulation study on potential new composite materials to moderate neutron-gamma radiation. Prog. Nucl. Energy **130**, 103538 (2020). https://doi.org/10.1016/j.pnucene.2020.103538
22. Brown, D.A.; Chadwick, M.B.; Capote, R.; Kahler, A.C.; Trkov, A.; Herman, M.W.; Sonzogni, A.A.; Danon, Y.; Carlson, A.D.; Dunn, M.; Smith, D.L.; Hale, G.M.; Arbanas, G.; Arcilla, R.; Bates, C.R.; Beck, B.; Becker, B.; Brown, F.; Casperson, R.J.; Conlin, J.; Cullen, D.E.; Descalle, M.-A.; Firestone, R.; Gaines, T.; Guber, K.H.; Hawari, A.I.; Holmes, J.; Johnson, T.D.; Kawano, T.; Kiedrowski, B.C.; Koning, A.J.; Kopecky, S.; Leal, L.; Lestone, J.P.; Lubitz, C.; Márquez Damián, J.I.; Mattoon, C.M.; McCutchan, E.A.; Mughabghab, S.; Navratil, P.; Neudecker, D.; Nobre, G.P.A.; Noguere, G.; Paris, M.; Pigni, M.T.; Plompen, A.J.; Pritychenko, B.; Pronyaev, V.G.; Roubtsov, D.; Rochman, D.; Romano, P.; Schillebeeckx, P.; Simakov, S.; Sin, M.; Sirakov, I.; Sleaford, B.; Sobes, V.; Soukhovitskii, E.S.; Stetcu, I.; Talou, P.; Thompson, I.; van der Marck, S.; Welser-Sherrill, L.; Wiarda, D.; White, M.; Wormald, J.L.; Wright, R.Q.; Zerkle, M.; Žerovnik, G.; Zhu, Y.: ENDF/B-VIII.0: the 8th major release of the nuclear reaction data library with CIELO-project cross sections, new standards and thermal scattering data. Nucl. Data Sheets **148**, 1–142 (2018). https://doi.org/10.1016/j.nds.2018.02.001
23. Cullen, D.E.: A survey of photon cross section data for use in EPICS2017, IAEA-NDS-225, rev.1 (2018)
24. Cullen, D.E.: EPICS2017: April 2019 status report, IAEA-NDS-228 (2019)
25. Basaglia, T.; Bonanomi, M.; Cattorini, F.; Choi, C.; Han, M.C.; Hoff, G.; Kim, C.H.; Hun Kim, S.; Marcoli, M.; Pia, M.G.; Saracco, P.: Assessment of new evaluated atomic data libraries in ENDF/B-VIII.0. In: 2018 IEEE Nuclear Science Symposium and Medical Imaging Conference Proceedings (NSS/MIC). IEEE (2018)
26. Kumar, A.: Gamma ray shielding properties of PbO–Li_2O–B_2O_3 glasses. Radiat. Phys. Chem. **136**, 50–53 (2017). https://doi.org/10.1016/j.radphyschem.2017.03.023
27. Sayyed, M.I.; Zaid, M.H.M.; Effendy, N.; Matori, K.A.; Sidek, H.A.A.; Lacomme, E.; Mahmoud, K.A.; AlShammari, M.M.: The influence of PbO and Bi_2O_3 on the radiation shielding and elastic features for different glasses. J. Mater. Res. Technol. **9**, 8429–8438 (2020). https://doi.org/10.1016/j.jmrt.2020.05.113
28. Bagheri, R.; Khorrami Moghaddam, A.; Yousefnia, H.: Gamma ray shielding study of barium–bismuth–borosilicate glasses as transparent shielding materials using MCNP-4C Code, XCOM program, and available experimental data. Nucl. Eng. Technol. **49**, 216–223 (2017). https://doi.org/10.1016/j.net.2016.08.013
29. Aşkın, A.; Sayyed, M.I.; Sharma, A.; Dal, M.; El-Mallawany, R.; Kaçal, M.R.: Investigation of the gamma ray shielding parameters of (100–x)[$0.5Li_2O$–$0.1B_2O_3$–$0.4P_2O_5$]–xTeO_2 glasses using Geant4 and FLUKA codes. J. Non-Cryst. Solids **521**, 119489 (2019). https://doi.org/10.1016/j.jnoncrysol.2019.119489
30. Sayyed, M.I.; El-Mesady, I.A.; Abouhaswa, A.S.; Askin, A.; Rammah, Y.S.: Comprehensive study on the structural, optical, physical and gamma photon shielding features of B_2O_3–Bi_2O_3–PbO–TiO_2 glasses using WinXCOM and Geant4 code. J. Mol. Struct. **1197**, 656–665 (2019). https://doi.org/10.1016/j.molstruc.2019.07.100
31. Sharma, A.; Sayyed, M.I.; Agar, O.; Tekin, H.O.: Simulation of shielding parameters for TeO_2–WO_3–GeO_2 glasses using FLUKA code. Results Phys. **13**, 102199 (2019). https://doi.org/10.1016/j.rinp.2019.102199
32. Aşkin, A.; Mutuwong, C.; Nutaro, T.; Dal, M.: Investigation of the radiation shielding capability of xPbO–(50–x)BaO–$50B_2O_3$ glass system using Geant4, Fluka, WinXCOM and comparison of data with the experimental data. Pramana J. Phys. (2019). https://doi.org/10.1007/s12043-019-1890-4
33. Trkov, A.; Herman, M.; Brown, D.A.: ENDF-6 formats manual: data formats and procedures for the evaluated nuclear data files, ENDF/B-VI and ENDF/B-VII, CSEWG Document ENDF-102, Report BNL-90365-2009 Rev. 2, Brookhaven National Laboratory (2009)
34. Hila, F.C.; Amorsolo, A.V., Jr.; Javier-Hila, A.M.V.; Guillermo, N.R.D.: A simple spreadsheet program for calculating mass attenuation coefficients and shielding parameters based on EPICS2017 and EPDL97 photoatomic libraries. Radiat. Phys. Chem. **177**, 109122 (2020). https://doi.org/10.1016/j.radphyschem.2020.109122